Comparison and Contrasts between the Active Site PKs of Mn-Superoxide Dismutase and Those of Fe-Superoxide Dismutase

James Maliekal,[†] Anush Karapetian,[†] Carrie Vance,[‡] Emine Yikilmaz,[†] Qiang Wu,[§]
Timothy Jackson,[‖] Thomas C. Brunold,[‖] Thomas G. Spiro,[§] and
Anne-Frances Miller*,[†,‡,⊥]

*Departments of Chemistry and Biochemistry, University of Kentucky,
Lexington, Kentucky 40506-0055, Jenkins Department of Biophysics, The Johns Hopkins
University, Baltimore, Maryland 21218, Department of Chemistry, Princeton University,
Princeton, New Jersey 08544, Department of Chemistry, University of Wisconsin,
1101 W. University Avenue, Madison, Wisconsin 53706, and Department of Chemistry,
The Johns Hopkins University, Baltimore, Maryland 21218*

Received June 17, 2002

Abstract: The Fe- and Mn-containing superoxide dismutases catalyze the same reaction and have almost superimposable active sites. Therefore, the details of their mechanisms have been assumed to be similar. However, we now show that the pH dependence of *Escherichia coli* MnSOD activity reflects a different active site proton equilibrium in (oxidized) Mn^{3+}SOD than the event that affects the active site pK of oxidized FeSOD. We find that the universally conserved Tyr34 that has a pK above 11.5 in Fe^{3+}SOD is responsible for the pK near 9.5 of Mn^{3+}SOD and, thus, that the oxidized state pK of Mn^{3+}SOD corresponds to an outer-sphere event whereas that of Fe^{3+}SOD corresponds to an inner sphere event [Bull, C.; Fee, J. A. *J. Am. Chem. Soc.* **1985**, *107*, 3295−3304]. We also present the first description of a reduced-state pK for MnSOD. Mn^{2+}SOD's pK involves deprotonation of Tyr34, as does Fe^{2+}SOD's pK [Sorkin, D. L.; Miller A.-F. *Biochemistry* **1997**, *36*, 4916−4924]. However, the values of the pKs, 10.5 and 8.5 respectively, are quite different and Mn^{2+}SOD's pK affects the coordination geometry of Mn^{2+}, most likely via polarization of the conserved Gln146 that hydrogen bonds to axially coordinated H_2O. Our findings are consistent with the different electronic configurations of $Mn^{2+/3+}$ vs $Fe^{2+/3+}$, such as the stronger hydrogen bonding between Gln146 and coordinated solvent in MnSOD than that between the analogous Gln69 and coordinated solvent in FeSOD, and the existence of weakly localized H_2O near the sixth coordination site of Mn^{2+} in Mn^{2+}SOD [Borgstahl et al. *J. Mol. Biol.* **2000**, *296*, 951−959].

Introduction

Fe- and the Mn-containing superoxide dismutases (FeSODs and MnSODs) catalyze the disproportionation of superoxide.[3−5] These two types of SOD bear no significant homology to the Cu- and Zn-containing SODs[6] or Ni-containing SODs,[7] but FeSODs and MnSODs are closely related to one another, sharing the same overall fold and high amino acid sequence identity.[2,8] In both, the active site metal ion is bound in trigonal bipyramidal geometry by three equatorial ligands: two histidines and one aspartate, and two axial ligands: a third His and a molecule of coordinated solvent (Figure 1). The axial coordinated solvent[9] hydrogen bonds with a conserved Gln (Gln69 in FeSOD, Gln146 in MnSOD)[10] which in turn hydrogen bonds with the universally conserved Tyr34, as well as a Trp and an Asn (Figure 1). Between Tyr34, Mn, the ligands His170, His81, His26 and surrounding residues Trp169, Trp85, His30, and His31 there is a cavity[11,12] in which the substrate analogue N_3^- binds,[2] and

* To whom correspondence should be addressed. E-mail: afm@pop.uky.edu. Tel: (859) 257-9349. Fax: (859) 323-1069.
† Departments of Chemistry and Biochemistry, University of Kentucky.
‡ Jenkins Department of Biophysics, The Johns Hopkins University.
§ Department of Chemistry, Princeton University, Princeton.
‖ Department of Chemistry, University of Wisconsin.
⊥ Department of Chemistry, The Johns Hopkins University.

(1) Borgstahl, G. E. O.; Pokross, M.; Chehab, R.; Sekher, A.; Snell, E. H. *J. Mol. Biol.* **2000**, *296*, 951−959.
(2) Lah, M. S.; Dixon, M. M.; Pattridge, K. A.; Stallings, W. C.; Fee, J. A.; Ludwig, M. L. *Biochemistry* **1995**, *34*, 1646−1660.
(3) Whittaker, J. W. In *Manganese and its Role in Biological Processes*; Sigel, A., Sigel, H., Eds.; Marcel Dekker: New York, 2000; Vol. 37, pp 587−611.
(4) Whittaker, J. W. In *Superoxide Dismutase*; Packer, L., Ed.; Academic Press: New York, 2002; Vol. 349, pp 80−90.
(5) Miller, A.-F. In *Handbook of Metalloproteins*; Wieghardt, K., Huber, R., Poulos, T. L., Messerschmidt, A., Eds.; Wiley and Sons: Chichester, 2001; Vol. 1, pp 668−682.
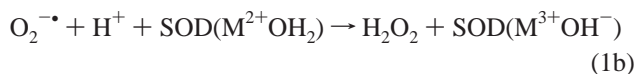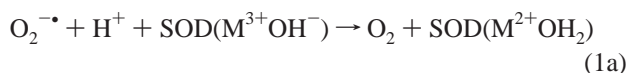
(6) Bordo, D.; Pesce, A.; Bolognesi, M.; Stroppolo, M. E.; Falconi, M.; Desideri, A. In *Handbook of Metalloproteins*; Wieghardt, K., Huber, R., Poulos, T. L., Messerschmidt, A., Eds.; Wiley and Sons: Chichester, 2001; Vol. 2, pp 1284−1300.
(7) Lee, J.-W.; Roe, J.-H.; Kang, S.-O. In *Superoxide Dismutase*; Packer, L., Ed.; Academic Press, New York, 2002; Vol. 349, pp 90−101.
(8) Smith, M. W.; Doolittle, R. F. *J. Mol. Evol.* **1992**, *34*, 175−184.
(9) We refer to the coordinated solvent in the axial position that hydrogen bonds with Gln146 as the "existing solvent" and the one that may add to the coordination sphere in the equatorial sixth position as "additional solvent" to distinguish between the two.
(10) Numbering of *Escherichia coli* FeSOD and MnSOD are used throughout.
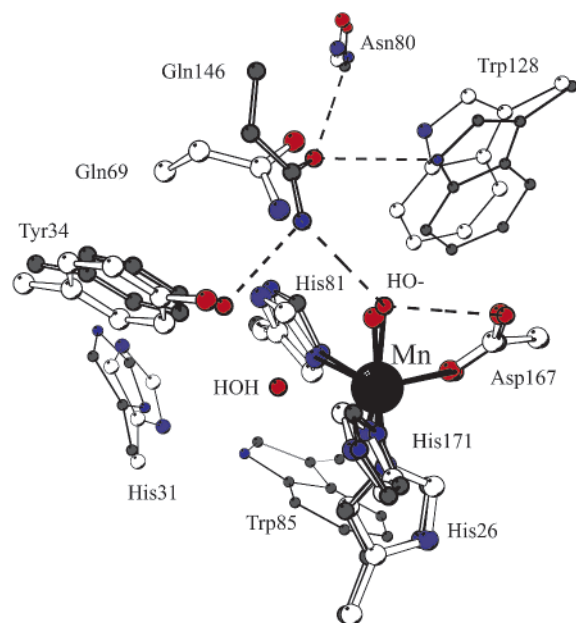
Figure 1. Overlay of the active sites of MnSOD and Fe^{3+}SOD based on the coordinates of [1] and [2], respectively. The Fe^{3+}SOD structure is drawn in light wide lines and the MnSOD structure in dark narrow lines. The FeSOD homologue of Trp85 is omitted for clarity and the numbering is only given for MnSOD residues, with the exception that FeSOD's Gln69 is also numbered.

an "additional" molecule of solvent is resolved at low temperature.[1]

MnSOD and FeSOD have both been shown by pulsed radiolysis to employ a two-stroke mechanism in which the metal ion, M = Fe or Mn, alternates between the 3+ and 2+ oxidation states,[13–16] and the existing coordinated solvent goes from being OH$^-$ in the oxidized state to H$_2$O in reduced SOD[14,17,18]

$$O_2^{-\bullet} + H^+ + SOD(M^{3+}OH^-) \rightarrow O_2 + SOD(M^{2+}OH_2)$$
(1a)

$$O_2^{-\bullet} + H^+ + SOD(M^{2+}OH_2) \rightarrow H_2O_2 + SOD(M^{3+}OH^-)$$
(1b)

where SOD signifies the protein. The activities of FeSOD and MnSOD both decrease at high pH,[14,19] both are inhibited by anions such as F$^-$ and N$_3^-$ [14,20,21] and both SOD proteins can bind either Fe or Mn.[22,23] However, details of the mechanism, such as the assignments of the pKs and proton coupling to electron transfer, are better known for FeSOD than for MnSOD,

so in the absence of experimental information, it has generally been assumed that the FeSOD mechanism applies to MnSOD as well. However, we believe that there are chemically significant differences between the two different protein environments as well as the intrinsic reactivities of the two metal ions.[24,25]

FeSOD and MnSOD differ subtly in a number of ways. (1) Stopped flow and pulsed radiolysis studies demonstrated that in addition to completing reaction 1b, the Mn^{2+}SOD–O$_2^{-\bullet}$ adduct also reorganizes to form an unproductive intermediate presumed to be a side-on Mn^{3+}–peroxo complex,[13,26,27] from which it recovers completely but slowly.[13,26–28] Conversely, FeSOD is irreversibly inactivated by HO$_2^-$ with concomitant Fe release and amino acid modification.[29–32] (2) Crystal structures of the N$_3^-$ complexes of Fe^{3+}SOD and Mn^{3+}SOD show N$_3^-$ bound at an angle to the Fe^{3+}-to-coordinating-N vector in Fe^{3+}SOD, but in Mn^{3+}SOD, it binds more linearly and engages in a hydrogen bond with Tyr34.[2] (3) F$^-$ binds to Fe^{2+}SOD outside the first coordination sphere,[33] whereas it joins the first coordination sphere in Mn^{2+}SOD based on EPR spectroscopy.[34] (4) The protein of MnSOD, (Mn)SOD, appears to depress the reduction midpoint potential (E_m) of the bound metal ion approximately half a volt more than does the protein of FeSOD, (Fe)SOD.[35,36]

The half-volt difference in redox tuning is striking, given the near-superimposability of the FeSOD and MnSOD active sites (Figure 1). We have proposed that this derives in large measure from different stabilization of metal-coordinated OH$^-$ relative to H$_2$O in the "existing" axial position in the two proteins,[24,35–37] via different hydrogen bonding with Gln69/146. Gln69/146 represents the most highly conserved difference between FeSODs and MnSODs[38,39] and is the existing coordinated solvent's only interaction with a group outside the ligand sphere (Figure 1). The Gln appears closer to coordinated solvent and more strongly coupled to it in *E. coli* MnSOD than that in *E. coli* FeSOD.[2,24,40,41]

Finally, two protons are required for turnover. Although these originate in bulk solvent, they are almost certainly supplied to substrate and/or nascent product by active site residues, including the existing coordinated solvent molecule. The active site

(11) Stallings, W. C.; Bull, C.; Fee, J. A.; Lah, M. S.; Ludwig, M. L. In *Molecular Biology of Free Radical Scavenging Systems*; Cold Spring Harbor: Plainview, New York, 1992.
(12) Ludwig, M. L.; Metzger, A. L.; Pattridge, K. A.; Stallings, W. C. *J. Mol. Biol.* **1991**, *219*, 335–358.
(13) McAdam, M. E.; Lavelle, F.; Fox, R. A.; Fielden, E. M. *Biochem. J.* **1977**, *165*, 81–87.
(14) Bull, C.; Fee, J. A. *J. Am. Chem. Soc.* **1985**, *107*, 3295–3304.
(15) Pick, M.; Rabani, J.; Yost, F.; Fridovich, I. *J. Am. Chem. Soc.* **1974**, *96*, 7329–7333.
(16) Lavelle, F.; McAdam, M. E.; Fielden, E. M.; Roberts, P. B.; Puget, K.; Michelson, A. M. *Biochem. J.* **1977**, *161*, 3–11.
(17) Han, W. G.; Lovell, T.; Noodleman, L. *Inorg. Chem.* **2002**, *41*, 205–218.
(18) Stallings, W. C.; Metzger, A. L.; Pattridge, K. A.; Fee, J. A.; Ludwig, M. L. *Free Rad. Res. Comms.* **1991**, *12–13*, 259–268.
(19) Terech, A.; Pucheault, J.; Ferradini, C. *Biochem. Biophys. Res. Commun.* **1983**, *113*, 114–120.
(20) Misra, H. P.; Fridovich, I. *Arch. Biochem. Biophys.* **1978**, *189*, 317–322.
(21) Slykhouse, T. O.; Fee, J. A. *J. Biological Chem.* **1976**, *251*, 5472–5477.
(22) Ose, D. E.; Fridovich, I. *J. Biol. Chem.* **1976**, *251*, 1217–1218.
(23) Yamakura, F. *J. Biochem.* **1978**, *83*, 849–857.

(24) Schwartz, A. L.; Yikilmaz, E.; Vance, C. K.; Vathyam, S.; Koder, R. L., Jr.; Miller, A.-F. *J. Inorg. Biochem.* **2000**, *80*, 247–256.
(25) Xie, J.; Yikilmaz, E.; Miller, A.-F.; Brunold, T. C. *J. Am. Chem. Soc.* **2002**, *124*, 3769–3774.
(26) Bull, C.; Niederhoffer, E. C.; Yoshida, T.; Fee, J. A. *J. Am. Chem. Soc.* **1991**, *113*, 4069–4076.
(27) Hearn, A. S.; Tu, C.; Nick, H. S.; Silverman, D. N. *J. Biol. Chem.* **1999**, *274*, 24 457–24 460.
(28) Hearn, A. S.; Stroupe, M. E.; Cabelli, D. E.; Lepock, J. R.; Tainer, J. A.; Nick, H. S.; Silverman, D. S. *Biochemistry* **2001**, *40*, 12 051–12 058.
(29) Meier, B.; Sehn, A. P.; Michel, C.; Saran, M. *Arch Biochem. Biophys.* **1994**, *313*, 296–303.
(30) Dooley, D. M.; Koras, J. F.; Jones, T. F.; Coti, C. E.; Smith, S. B. *Inorg. Chem.* **1986**, *25*, 4761–4766.
(31) Beyer, J., W. F.; Fridovich, I. *Biochemistry* **1987**, *26*, 1251–1257.
(32) Yamakura, F. *Biochem. Biophys. Res. Commun.* **1984**, *122*, 635–641.
(33) Sorkin, D. L., Ph. D. Thesis, The Johns Hopkins University (1999).
(34) Whittaker, J. W.; Whittaker, M. M. *J. Am. Chem. Soc.* **1991**, *113*, 5528–5540.
(35) Vance, C. K.; Miller, A.-F. *J. Am. Chem. Soc.* **1998**, *120*, 461–467.
(36) Vance, C. K.; Miller, A.-F. *Biochemistry* **2001**, *40*, 13 079–13 087.
(37) Yikilmaz, E.; Xie, J.; Miller, A.-F.; Brunold, T. C. *J. Am. Chem. Soc.* **2002**, *124*, 3482–3483.
(38) Parker, M. W.; Blake, C. C. F. *FEBS Lett.* **1988**, *229*, 377–382.
(39) Carlioz, A.; Ludwig, M. L.; Stallings, W. C.; Fee, J. A.; Steinman, H. M.; Touati, D. *J. Biol. Chem.* **1988**, *263*, 1555–1562.
(40) Edwards, R. A.; Baker, H. M.; Jameson, G. B.; Whittaker, M. M.; Whittaker, J. W.; Baker, E. N. *J. B. I. C.* **1998**, *3*, 161–171.
(41) Edwards, R. A.; Whittaker, M. M.; Whittaker, J. W.; Jameson, G. B.; Baker, E. N. *J. Am. Chem. Soc.* **1998**, *120*, 9684–9685.

Scheme 1. Comparison of the Events Responsible for the PKs of the Active Sites of FeSOD and MnSOD, in Both Oxidation States
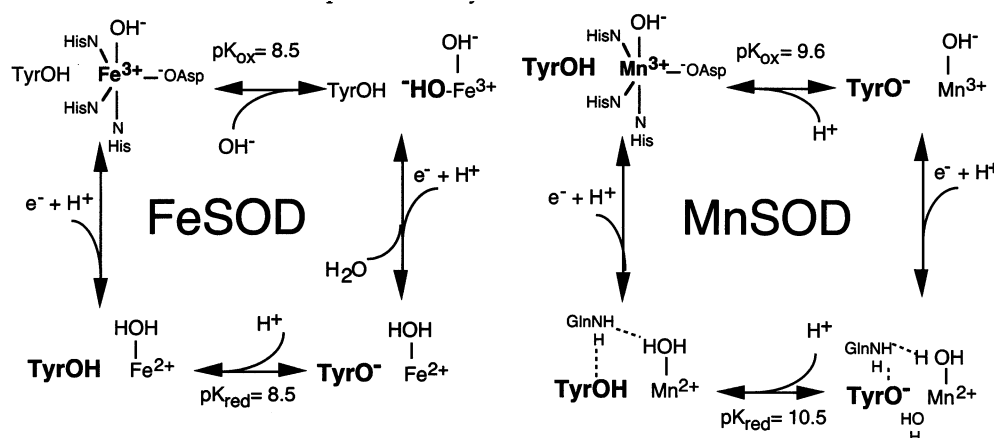
The four protein ligands appear coordinated in all states but are omitted in three states of each SOD for clarity. Proton uptake coupled to reduction is assumed for MnSOD by analogy with FeSOD. The "existing" axial coordinated solvent present in all states is positioned above the metal ion and in MnSOD derives a hydrogen bond from Gln146. When relevant, an additional equatorial solvent near the sixth coordination site is also shown to the metal ion's left, near Tyr34.

pKs associated with loss of activity at high pH have been assigned in FeSOD to binding of an additional OH^- as a sixth ligand to Fe^{3+} in the oxidized state (p$K = 8.6-9.0$ [14,42]) and ionization of Tyr34 in the reduced state (p$K = 8.5$,[43,44] Scheme 1). Human $Mn^{3+}SOD$'s pK near 9.5 has been attributed by Silverman to ionization of Tyr34 based on the pK's proximity to the pK of 10.5 of free Tyr and its perturbation by mutation of Tyr34 to Phe,[45,46] by Whittaker to additional OH^- binding to Mn^{3+} by analogy with $Fe^{3+}SOD$ but with retention of pentacoordination [47] and by Borgstahl to additional OH^- binding as an equatorial sixth ligand on the basis of observation of crystallographic solvent positioned so as to be coordinated to Mn at pH 8.5 and 100 K [1]. The pH dependence of the reduced state of MnSOD has not been published.

Given the potential importance to activity of labile active site protons, it is crucial to assign the active site pKs in MnSOD for comparison with those of FeSOD. Therefore, we now report a detailed spectroscopic assignment and characterization of the pH dependence of the active site of MnSOD. We assign $Mn^{3+}SOD$'s pK near 9.5 to ionization of Tyr34 and $Mn^{2+}SOD$'s pK near 10.5 to deprotonation of Tyr34 tentatively associated with effective partial deprotonation of axial coordinated H_2O. These assignments, as well as the values of the pKs, contrast with those established for FeSOD (Scheme 1). Thus, our results demonstrate that the active sites of FeSOD and MnSOD differ qualitatively as well as quantitatively with respect to OH^- binding and deprotonation of Tyr34. These findings suggest that the similar overall mechanisms of FeSOD and MnSOD may be accomplished in subtly different ways by the different enzymes, and support the possibility that the different redox tuning exerted by the two sites may stem to a significant extent from distinct distributions of labile proton density in the active site.

Materials and Methods

Proteins and Optical pH Titrations. MnSOD was overexpressed from the *sodA-, sodB- E. coli* strain QC774 transformed with the sodA gene on plasmid pDT1-5 [48] or pALS1/HMS174 [24] and purified as described previously.[35,49] The Y34F mutant gene was constructed using the megaprimer method,[50] and the sequence confirmed by sequencing both DNA strands. Y34F−MnSOD was overexpressed from the Δ*sodA,* Δ*sodB E. coli* strain Ox326A, kindly provided by Prof. H. Steinman.[51] Specific activities of >6000 units/mg·min for WT and 4800 units/mg· min for Y34F were typically obtained, as determined using the standard xanthine oxidase/cytochrome *c* assay.[52] Protein concentrations were determined using $\epsilon_{280} = 86\,600\ M^{-1}\ cm^{-1}$,[53] the concentration of active sites containing Mn^{3+} was determined using the WT-$Mn^{3+}SOD$ ϵ_{478} of $850\ M^{-1}\ cm^{-1}$ and the Y34F−$Mn^{3+}SOD$ value of $780\ M^{-1}\ cm^{-1}$.[47]

To facilitate NMR observation of the ζ carbon of Tyr side chains, these were selectively labeled with ^{13}C. Bacterial cultures were grown in M9 minimal medium supplemented with 1 g/l glyphosate to inhibit biosynthesis of aromatic amino acids,[54] as well as 50 mg/l Trp, 35 mg/l Phe and 50 mg/l $^{13}C^{\zeta}$-Tyr to support protein synthesis. Overexpression was induced with 1 mM IPTG when A_{600} reached 1 and cultures were harvested 3 h later. The protein was purified and manipulated as usual.[35,49]

Optically detected pH titrations were performed in a Hewlett-Packard 8452A diode array spectrophotometer equipped with a thermostated cell compartment. The pH was measured continuously using a combination pH microelectrode in a 12 gauge stainless steel needle (Microelectrodes Inc.), the pH was raised in small steps using 100 mM KOH and the optical spectrum was collected at each pH. Reversibility was confirmed by dialyzing samples against neutral pH buffer, or addition of an equal volume of 50 mM pH 7.0 phosphate buffer, because MnSOD was found to be relatively intolerant of addition of concentrated acid. pKs were obtained from fits to the data of the Henderson− Hasselbalch equation $(A_A - A_{obs})/(A_A - A_B) = (K)/(K + 10^{-(pH)})$ where A_A and A_B are the absorbances at 478 nm of the acid and base forms (the asymptotes obtained from the fit), A_{obs} is the observed absorbance at a given pH, K is the acid dissociation constant obtained from the fit and the Hill coefficient is set to 1.

(42) Tierney, D. L.; Fee, J. A.; Ludwig, M. L.; Penner-Hahn, J. E. *Biochemistry* **1995**, *34*, 1661−1668.
(43) Sorkin, D. L.; Miller, A.-F. *Biochemistry* **1997**, *36*, 4916−4924.
(44) Sorkin, D. L.; Duong, D. K.; Miller, A.-F. *Biochemistry* **1997**, *36*, 8202− 8208.
(45) Hsu, J.-L.; Hsieh, Y.; Tu, C.; O'Connor, D.; Nick, H. S.; Silverman, D. N. *J. Biol. Chem.* **1996**, *271*, 17 687−17 691.
(46) Guan, Y.; Hickey, M. J.; Borgstahl, G. E. O.; Hallewell, R. A.; Lepock, J. R.; O'Connor, D.; Hsieh, Y.; Nick, H. S.; Silverman, D. N.; Tainer, J. A. *Biochemistry* **1998**, *37*, 4722−4730.
(47) Whittaker, M. M.; Whittaker, J. W. *Biochemistry* **1997**, *36*, 8923−8931.

(48) Carlioz, A.; Touati, D. *EMBO J.* **1986**, *5*, 623−630.
(49) Vance, C. K.; Miller, A.-F. *Biochemistry* **1998**, *37*, 5518−5527.
(50) Barik, S. *Methods Mol. Biol.* **1996**, *67*, 173−182.
(51) Steinman, H. M. *Mol. Gen. Genet.* **1992**, *232*, 427−430.
(52) McCord, J. M.; Fridovich, I. *J. Biol. Chem.* **1969**, *244*, 6049−6055.
(53) Whittaker, M. M.; Whittaker, J. W. *Biochemistry* **1996**, *35*, 6762−6770.
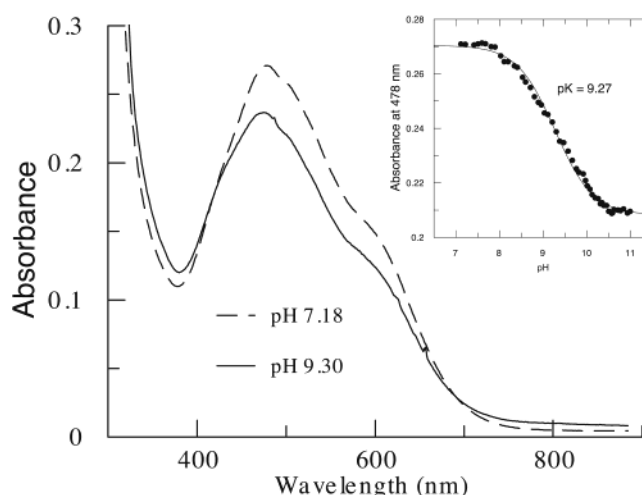(54) Kim, H. W.; Perez, J. A.; Ferguson, S. J.; Campbell, I. D. *FEBS Lett.* **1990**, *272*, 34−36.

Circular Dichroism. CD and MCD spectra were collected at a range of temperatures using a Jasco J-715 spectropolarimeter with an Oxford Instruments SM-4000 8T magnetocryostat. Samples contained approximately 1 mM MnSOD. Samples used in collection of low-temperature spectra contained glycerol at 55% v/v, and the pH was checked after addition of glycerol. Neutral pH samples were buffered at pH 7.0 with 50 mM potassium phosphate and high pH samples were at pH 11.0 in 100 mM CAPS (concentrations prior to dilution with glycerol).

NMR. NMR samples contained approximately 30 mg of MnSOD in 0.6 mL, resulting in dimer concentrations of approximately 1.1 mM. The samples for the pH titration were extensively dialyzed vs deionized water and ^2H_2O was included to a final concentration of 10% v/v. For each point in the titration the pH was adjusted using 100 mM KOH and measured using a combination pH microelectrode. At each pH two ^{13}C NMR spectra were collected. In addition to a nonselective NMR spectrum of all ^{13}Cs, we collected a spectrum selective for fast-relaxing nuclei in order to specifically observe Tyr34 and avoid confusing its resonance with overlapping sharper resonances. The pH dependence of the chemical shift of Tyr34 was fit to a Henderson−Hasselbalch equation with allowance for cooperativity:[55] $(\delta_A - \delta_{obs})/(\delta_A - \delta_B) = (10^{-n*pK})/(10^{-n*pK} + 10^{-n(pH)})$ in which δ_A and δ_B are the chemical shifts of the acid and base forms (the asymptotes obtained from the fit), δ_{obs} is the observed chemical shift at a given pH, pK is $-\log (K)$ where K is the acid dissociation constant obtained from the fit, and n is the Hill coefficient obtained from the fit. The pH dependencies of two other resolved Tyr $^{13}C^\zeta$ resonances that responded significantly to pH change within our range of study were fit to a Henderson−Hasselbalch equation without allowance for cooperativity ($n = 1$) and assuming an 8 ppm change in δ because the pH dependence was not large enough to warrant a three-parameter fit.

^{13}C NMR spectra were collected at 150 MHz on an Inova 600 MHz spectrometer, using a broadband 5-mm probehead to observe samples containing approximately 1 mM Mn^{3+}SOD. Nonselective spectra were collected using a 1 s recycle delay between scans, a 4 μs 30° excitation pulse, and 1 s of acquisition over a 45 kHz spectral range centered at 140 ppm. Spectra emphasizing paramagnetically relaxed resonances of Tyr C$^\zeta$s near Mn^{3+} were obtained by first saturating the sharper, and therefore taller, nonparamagnetically relaxed resonances that conceal them. This was achieved using WET [56,57] methodology, in which a series of 90° pulses selective for the Tyr $^{13}C^\zeta$ region were interspersed with Z-axis gradient pulses to randomize all Tyr C$^\zeta$ magnetization and achieve essentially complete presaturation. A short delay of 2 ms was then allowed for instrument stabilization prior to a 90° observation pulse and data acquisition. The recycle delay and acquisition time were restricted to 1 ms and 200 ms, respectively, to further emphasize paramagnetically relaxed ^{13}C magnetization. All chemical shifts are relative to external DSS at 0 ppm, and all spectra were collected at 25 °C.

EPR. EPR samples consisted of 250 μL of MnSOD reduced with slightly suprastoichiometric dithionite. pH titrations were performed with the same results in the absence of buffer, in the presence of 50 mM potassium phosphate or in the presence of 50 mM CAPS. Samples were adjusted to the desired pH prior to reduction and the pH was measured again after reduction. Very high pH samples required slight further pH adjustment after reduction due to H$^+$ release upon oxidation of dithionite. Samples were frozen promptly in liquid N$_2$, and EPR spectra were recorded at 65 or 110 K at X band using a Bruker 300MX spectrometer, an Oxford 900 cryostat, and liquid N$_2$ as the coolant. Spectra were collected at 9.47 GHz and a nominal power of 80 mW in 5000 G wide scans centered at 2500 G with 2 G modulation. Signal amplitudes at a series of positions in the spectrum were plotted as

(55) Markley, J. L. *Acc. Chem. Res.* **1975**, *8*, 70−80.
(56) Ogg, R. J.; Kingsley, P. B.; Taylor, J. S. *J. Magn. Reson. B* **1994**, *104*, 1.
(57) Smallcombe, S. H.; Patt, S. L.; Keiger, P. A. *J. Magn. Reson. A* **1995**, *117*, 295.

Figure 2. Optical spectrum of Mn^{3+}SOD at low and high pH, with inset pH titration of the absorbance at 478 nm, yielding pK = 9.27 ± 0.06.

functions of pH and the pK evaluated from fits with the Henderson−Hasselbalch equation neglecting cooperativity (above).

Resonance Raman. Samples consisted of approximately 1 mM Mn^{2+}SOD or Y34F Mn^{2+}SOD in a buffer cocktail composed of 10 mM HEPES (pK = 7.6), 10 mM Ala (pK$_2$ = 9.1) and 10 mM CAPS (pK = 10.4) designed to cover the pH range of 6.6 to 11.4. Individual samples were adjusted to the desired pH with 100 mM KOH using a combination microelectrode. The samples were reduced with a 2-to-3-fold stoichiometric excess of dithionite, and the pH was checked and adjusted again if necessary before flash freezing in dry ice/acetone. Samples were kept frozen until use, within a week. Duplicate samples were examined by low-temperature EPR.

An intracavity frequency-doubled CW Ar laser (Coherent FreD) was used for Raman excitation at 238 nm. UV resonance Raman spectra were acquired with a Spex 1269 single monochromator equipped with a CCD detector (Princeton Instruments). The samples were contained in a suprasil quartz NMR tube, which was spun around a stationary helical stir wire at ∼10 Hz for vertical mixing of the ∼300-μL sample.[58] The UV power at the surface of the sample tube was 1.1 mW (with a beam diameter of about 40 μm). Each spectrum was summed over 5 exposures of 60 s each. Three successive spectra were obtained at different NMR tube heights and were averaged to improve signal-to-noise. A spectrum of acetone obtained under identical conditions was used for frequency calibration. Intensities of Tyr bands at 1618 and 1602 cm^{-1} were obtained by peak deconvolution and curve fitting using GRAMS/32 (Galactic Industries Corp., Salem NH). The Trp band at 1010 cm^{-1} was used to normalize different pH spectra based on our experience that this band is relatively insensitive to environmental effects.

Results and Discussion

Assignment of the *p*K of Oxidized Mn^{3+}SOD. The optical spectrum of Mn^{3+}SOD at high pH is slightly different from that at neutral pH (see refs 46 and 47 Figure 2). A plot of the absorbance at 478 nm vs. pH reveals a well-behaved titration described by a single proton-equivalent event with a pK of 9.3 ± 0.1, consistent with earlier reports (pK=10.1,[46] pK=9.7,[47] pK = 9.4,[45] pK=9.8 [19]). However, the changes associated with the pK are subtle, and moreover much smaller than the effects induced by binding of N$_3^-$,[34,53] which is thought to bind in the inner sphere displacing the ligand Asp$^-$ at room temperature,

(58) Rodgers, K. R.; Su, C.; Subramaniam, S.; Spiro, T. G. *J. Am. Chem. Soc.* **1992**, *114*, 3697.
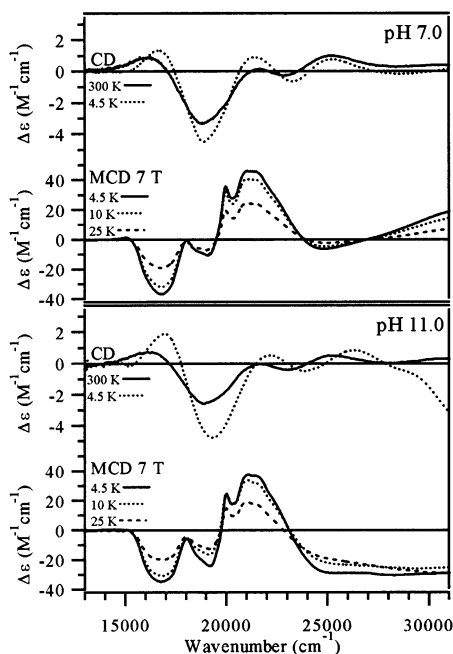
**Figure 3.** Comparison of the CD and MCD spectra of $Mn^{3+}SOD$ at pH 7 (top panel) and pH 11 (bottom panel). For each, CD spectra collected at room and low temperature (above) are compared with the MCD spectra obtained at three low temperatures (below).

but expanding the coordination sphere to hexacoordinate below 210 K.[53] Thus, it seems unlikely that at high pH, OH^- binds to Mn^{3+} in a similar manner as N_3^-.

Our MCD spectra indicate that at high pH $Mn^{3+}SOD$ is not hexacoordinate, since it lacks a band near 10 000 cm^{-1}, which is diagnostic of 6-fold coordination for Mn^{3+}.[34,53] Moreover, no such band is evident even at 4.5 K (Figure 3). In addition, our CD spectra indicate that the Mn^{3+} electronic structure is similar at room and low temperatures, arguing against a change in the nature of the pH event with temperature. (Some blue shifting and band sharpening are evident upon cooling, especially for the high pH sample. These are commonly consequences of low temperature depopulation of vibrational excited states, in combination with anharmonic potentials. The larger magnitudes of these effects for the high pH sample are consistent with softer potentials or the existence of an additional mode that is thermally excited at room temperature.) Thus, the room-temperature assignment should hold for temperatures down to 4.5 K and should not involve expansion of the coordination sphere (also see ref 47). If OH^- binds and the Mn^{3+} remains pentacoordinate due to displacement of the Asp^- ligand, as proposed for N_3^- binding at room temperature,[53] the charge transfer region of the MCD spectrum should be strongly perturbed, but this is not observed. Alternatively, displacement of the existing OH^- ligand would produce a square pyramidal site and therefore give rise to large shifts in the d−d transitions, which is also not observed. Thus, the event responsible for the pK near 9.5 most likely corresponds to an outer sphere event.

The most likely outer-sphere candidate for the pK near 9.5 is ionization of Tyr34. Therefore, we have incorporated ^{13}C specifically in the C^ζ position of the Tyrs of $Mn^{3+}SOD$. This is the position closest to the ionizable OH and it typically displays an 8−10 ppm downfield shift of its NMR resonance upon deprotonation of the phenolic OH.
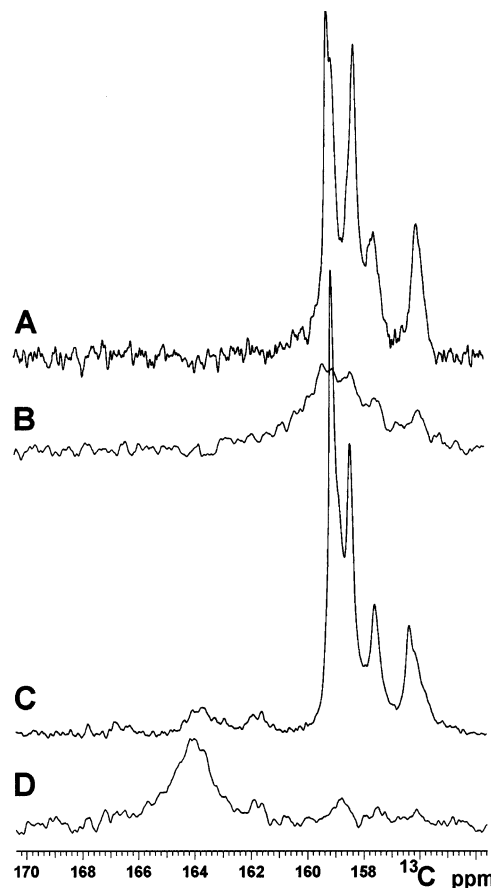

Figure 4. ^{13}C NMR spectra of $Mn^{3+}SOD$ Tyr C^ζ resonances. A and B were collected at pH 6.1 and C and D were collected at pH 10.6. A and C are unbiased spectra of all Cs whereas B and D are spectra obtained after WET suppression of resonances whose relaxation is not accelerated by paramagnetism. Thus, spectra B and D reflect primarily the resonance of Tyr34. Spectra A and C were processed with 10 Hz Lorentz line broadening whereas 20 Hz line broadening was used for B and D. Other details are provided in the Methods section.

[Tyr $^{13}C^\zeta$]-$Mn^{3+}SOD$ displays approximately 50-fold specific enhancement of the signals of Tyr C^ζs, between 154 and 162 ppm (not shown). Deconvolution of this spectral region reveals the presence of six resonances with comparable T_1s, corresponding to all but one of the seven Tyrs in MnSOD (Figure 4A). When this spectral region is saturated, the six resonances are almost completely suppressed and a seventh much broader underlying resonance is revealed at 159 ppm (Figure 4B). Since Tyr34's C^ζ is only 5.7−5.9 Å from Mn but all the other Tyr C^ζs are 8.5 Å or more away,[1,40] Tyr34 is expected to be much more severely paramagnetically relaxed than the other Tyrs. This is consistent with the 159 ppm resonance's obviously broader line width and its much shorter T_1. Therefore, this resonance is assigned to Tyr34.

A similar pair of spectra collected at pH 10.6, above the pK, reveal small changes in the positions of the nonparamagnetically relaxed ("diamagnetic") resonances but a large displacement of the resonance of Tyr34, in a direction consistent with deprotonation of Tyr34 (Figure 4, C & D). Tyr34's resonance may also sharpen slightly, but the effect is not large and is obscured by residual intensity of diamagnetic signals at neutral pHs.

The pH dependence of Tyr34's $^{13}C^\zeta$ chemical shift as well as those of representative resolved diamagnetic resonances are
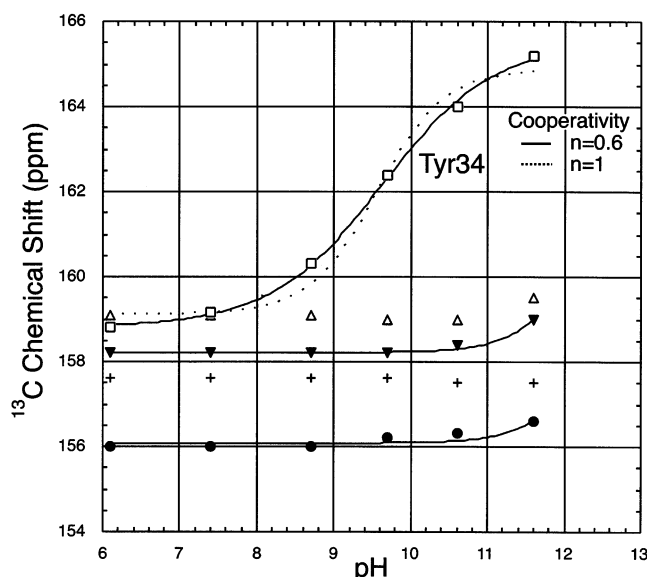
Figure 5. pH titrations of Tyr $^{13}C^\zeta$ resonances of Mn^{3+}SOD at 25 °C. Chemical shifts relative to external DSS are plotted for each of five resonances that were resolved throughout the pH range. q denotes the chemical shift of the resonance assigned to Tyr34, and the other resonances are as yet unassigned. Dotted line: fit with the Henderson Hasselbalch equation neglecting cooperativity, which yields a pK of 9.5 ± 0.2, solid line: fit with the Henderson Hasselbalch equation incorporating anti-cooperativity of $n = 0.6$, which yields a pK of 9.6 ± 0.06. The ● and ▼ resonances' pH titrations begin to titrate at high pH and can be described by pKs of 12.7 and 12.6 respectively, assuming a chemical shift change of 8 ppm and no cooperativity.

shown in Figure 5. Two of the diamagnetic Tyrs are beginning to titrate at the high end of the pH range in which Mn^{3+}SOD is stable, consistent with the tendency of free Tyr to titrate at pHs near 10.5 and the fact that the Tyrs of MnSOD are substantially buried. In contrast, Tyr34's chemical shift is described by a single pK of 9.6 ±.1. This pK is very close to the active site pK revealed by the optically detected pH titration, and suggests that the same event is being observed by NMR. Thus, we assign the active site pK near 9.5 to deprotonation of Tyr34.

To obtain the best fit to the NMR data it was necessary to incorporate effects of cooperativity. The Hill coefficient obtained, $n = 0.6$, suggests that the observed event is anti-cooperative with another pH-dependent event, although this is not evident in the optical pH transition. Deprotonation of Tyr34 can account for the attenuation and slight shifts in the optical signal observed at high pH, as ionization of Tyr34 would constitute a significant change in Mn^{3+}'s local dielectric, which is expected to alter the intensities of electric-dipole-mediated transitions to varying extents, depending on the orientations of their transition dipoles.

Relation to Previous Results. MnSOD has been known to have a pK near 9.5 since 1983.[19] Although it was shown to affect K_M rather than k_{cat}, the identity of the event(s) responsible had not previously been identified experimentally. Our assignment of the pK of oxidized Mn^{3+}SOD to ionization of Tyr34 confirms the earlier hypotheses of Silverman,[45] Parker and Blake,[59] and is consistent with strong perturbation of the pH behavior in mutants of Tyr34.[46,47,60]

This assignment can be reconciled with the 100 K crystal structure of MnSOD[1] because the crystal's pH of approximately 8.5 suggests that only 10% or less of the Mn^{3+} sites are in the high pH form. This argues that the additional solvent in the equatorial position is most likely H$_2$O, not OH$^-$, and is consistent with the significantly longer Mn−O bond for the additional solvent (2.42 (0.01) Å) when compared with the bonds to other ligands (2.19 (0.02) Å for the existing coordinated solvent).[1] Significantly weaker bonding to Mn^{3+} is also indicated by the absence of an MCD band near 10 000 cm^{-1}, and the reported low occupancy of 20−43%[1]. Finally, the crystal structure most likely represents a mixture of oxidation states, of which we argue that the reduced (Mn^{2+}) sites are most likely the ones with an additional equatorial H$_2$O bound (see below). Thus, we propose that the low-occupancy equatorial solvent molecule reflects primarily H$_2$O bound to Mn^{2+} sites (not observed by the MCD or NMR spectra), and is not a signature of the high-pH state of Mn^{3+}SOD.

The pK of Mn^{3+}SOD has also been proposed to correspond to binding of OH$^-$ to Mn^{3+} with retention of 5-coordinate ligation[47] due to displacement of coordinated Asp$^-$ (or existing OH$^-$) as proposed for N$_3^-$ binding.[53] In the case of N$_3^-$ binding, ligand Asp$^-$ (or OH$^-$) is proposed to be protonated upon displacement from Mn^{3+}.[47,53] N$_3^-$ + H$^+$ + Mn^{3+}(OH$^-$)(Asp$^-$) → (N$_3^-$)Mn^{3+}(OH$^-$) + HAsp (or (N$_3^-$)Mn^{3+}(Asp$^-$) + H$_2$O). The required uptake of a proton in conjunction with anion binding is consistent with decreased anion binding at high pH.[47] However, the same model cannot explain the pK in terms of OH$^-$ binding because this would not increase at high pH, as the net reaction would involve H$^+$ as well as OH$^-$. If the proton required for dissociation of Asp$^-$ or OH$^-$ were obtained internally rather than by net H$^+$ uptake, i.e., from Tyr34, then this proposed high pH event would also de facto correspond to ionization of Tyr34, as we propose.

However, there may be little energetic motivation for proton transfer from Tyr34 to dissociating Asp$^-$ or OH$^-$ ligands. The pK of Asp is normally lower than that of Tyr and such a rearrangement would also incur the cost of dissociating Asp. The other proposed rearrangement amounts to displacement by incoming additional OH$^-$ of an existing (and thus tighter-binding) coordinated OH$^-$ that appears significantly stabilized by hydrogen bonding from Gln146. Thus, neither of the scenarios invoking binding of OH$^-$ to Mn^{3+} with proton transfer from Tyr34 to a leaving ligand seems thermodynamically favorable. Instead, we propose that the high pH transition corresponds to ionization of Tyr34 and that this inhibits anion binding at high pH because Tyr34 is at the base of the substrate binding channel [2]. Therefore, at high pH, incoming anions are either subject to electrostatic repulsion by Tyr34$^-$ or fail to bind due to loss of favorable interactions mediated by Tyr34's ionizable proton (for example a hydrogen bond).[61]

Identification of a pK Affecting the Reduced State and its Assignment to Tyr34. The pH dependence of Mn^{2+}SOD has not previously been addressed in the literature. However, the active site of Fe^{2+}SOD exhibits a pK corresponding to deprotonation of Tyr34.[43,44] Therefore, we have characterized the pH dependence of the active site of (reduced) Mn^{2+}SOD

(59) Parker, M. W.; Blake, C. C. F. *J. Mol. Biol.* **1988**, *199*, 649−661.
(60) Edwards, R. A.; Whittaker, M. M.; Whittaker, J. W.; Baker, E. N.; Jameson, G. B. *Biochemistry* **2001**, *40*, 15−27.

(61) Alternately, deprotonated Tyr34 would draw H$^+$ density from Gln146 and decrease Gln146's ability to donate H$^+$ density to existing coordinated solvent and so facilitate dissociation as OH$^-$ when N$_3^-$ binds. Indeed, mutation of Gln146 abolishes anion binding (ref 60).
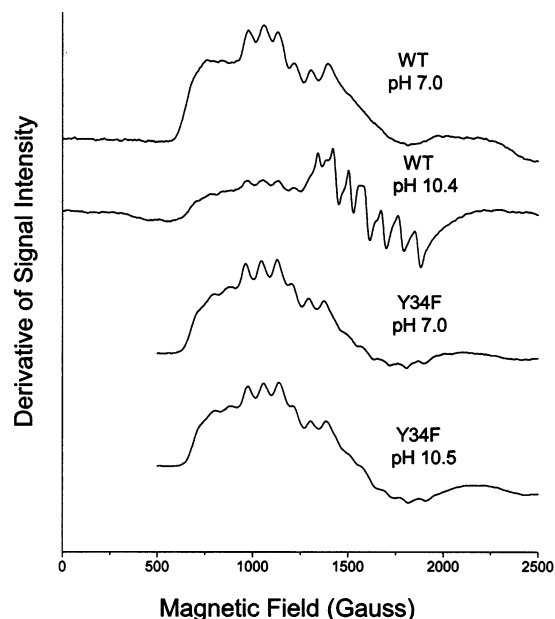
Figure 6. Low-field EPR signals of $Mn^{2+}SOD$ at low and high pH, for WT- and Y34F−$Mn^{2+}SOD$. EPR parameters are listed in the Methods section. A small signal from residual Fe^{3+} is visible near 1500 G, especially in high pH WT-$Mn^{2+}SOD$.
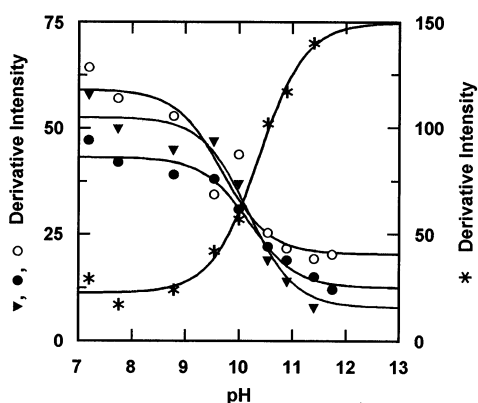

Figure 7. pH titration of features of the low and high pH EPR signals of $Mn^{2+}SOD$. The amplitudes of the low pH features at 725 G, 900 and 1125 G are denoted by ●, ○ and ▼, respectively and the amplitude of a high-pH feature, at 1400 G is plotted vs. pH as ∗. The pKs obtained for these from fits with the Henderson Hasselbalch equation are 10.2, 9.7, 10.2, and 10.4, respectively.

by resonance Raman observation of Tyrs at room temperature and EPR spectroscopy of Mn^{2+} at low temperature.

Figure 6 shows that WT-$Mn^{2+}SOD$ samples at high and low pH display distinct Mn^{2+}-derived EPR signals (identified by their characteristic ^{55}Mn hyperfine splittings of ∼90 G). The amplitudes of various Mn^{2+} features are plotted vs pH in Figure 7. Fits with the Henderson−Hasselbalch equation for a single proton pH equilibrium yield an average pK of 10.2 ± 0.3. Because the event significantly affects the EPR spectrum, it most likely affects the Mn^{2+} coordination sphere. However, the fact that this event is altered by mutation of Tyr34 strongly implicates that residue as well.

To obtain a definitive assignment of the pK, we used resonance Raman spectroscopy to directly observe Tyr residues, as well as to address the possibility that the pK might depend on temperature. Figure 8 shows UV resonance Raman spectra obtained upon excitation at 238 nm, which specifically enhances
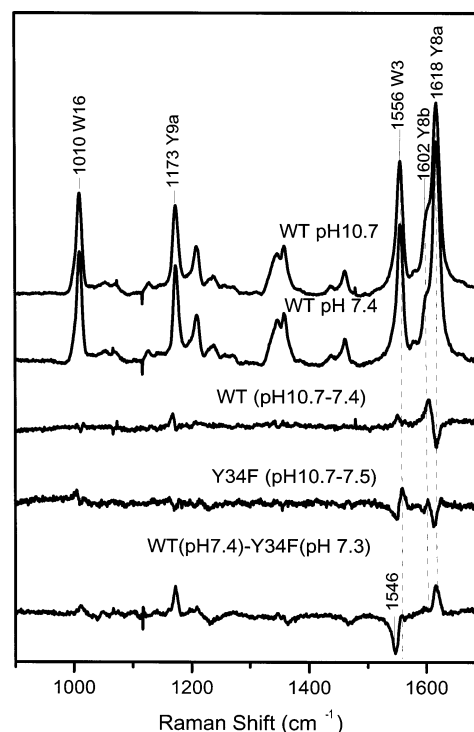
Figure 8. 238 nm-excited resonance Raman spectra of $Mn^{2+}SOD$ (0.5 mM) at pHs 7.4 and 10.7, and the difference spectrum, obtained using the 1010 cm^{-1} Trp band as an internal reference. Also shown is the corresponding high-minus-low pH difference spectrum for the Y34F mutant (0.54 mM), and the neutral pH difference spectrum between WT- and Y34F-$Mn^{2+}SOD$ (after adjustment of the overall intensities for the slightly different SOD concentrations). Prominent bands arising from Tyr (Y8a,b, Y9) and Trp (W3, W16) modes are labeled.[62,63]

vibrational modes of Tyr and Trp.[62,63] When spectra obtained at pH 7.4 and 10.7 are compared, using the 1010 cm^{-1} Trp W16 band as an internal reference, the only significant change is intensity loss at 1618 cm^{-1} and gain at 1602 cm^{-1}. This change reflects Tyr ionization because the 1618 cm^{-1} Y8a band occurs at 1602 cm^{-1} in tyrosinate (Tyr^-), coincident with the weaker Y8b band of neutral Tyr. The shift from Tyr to Tyr^- is shown clearly in the positive and negative difference bands in the pH 10.7−7.4 difference spectrum. When the same spectral subtraction is performed for mutant Y34F−$Mn^{2+}SOD$, a similar, but attenuated pair of difference features is observed. Thus, a substantial amount of the Tyr ionization at high pH in WT-$Mn^{2+}SOD$ is ascribed to Tyr34.

In Y34F−$Mn^{2+}SOD$, a Trp also responds to pH as revealed by a derivative feature at the position of the 1556 cm^{-1} W3 band. The frequency of this mode is known to be sensitive to changes in the dihedral angle, χ^2, between the indole ring and the C^β atom of the Trp residue.[64] Thus, a deprotonation event produces a change in this angle for one or more of the six Trp residues in $Mn^{2+}SOD$.

The Y34F mutation itself produces an alteration of the Trp W3 band, as seen in the pH 7.3 difference spectrum between WT and Y34F−$Mn^{2+}SOD$. In addition to the positive Tyr

(62) Austin, J. C.; Jordan, T.; G., S. T. In *Advances in Spectroscopy*; Clark, R. J. H., Hester, R. E., Eds.; John Wiley and Sons: New York, 1993; Vol. 20−21, pp 55.

(63) Harada, I.; Takeuchi, H. In *Advances in Spectroscopy*; Clark, R. J. H., Hester, R. E., Eds; John Wiley and Sons: New York, 1993; Vol. 20−21, pp 113.

(64) Miura, T.; Takeuchi, H.; Harada, I. *J. Raman Spectrosc.* **1989**, *20*, 667−671.
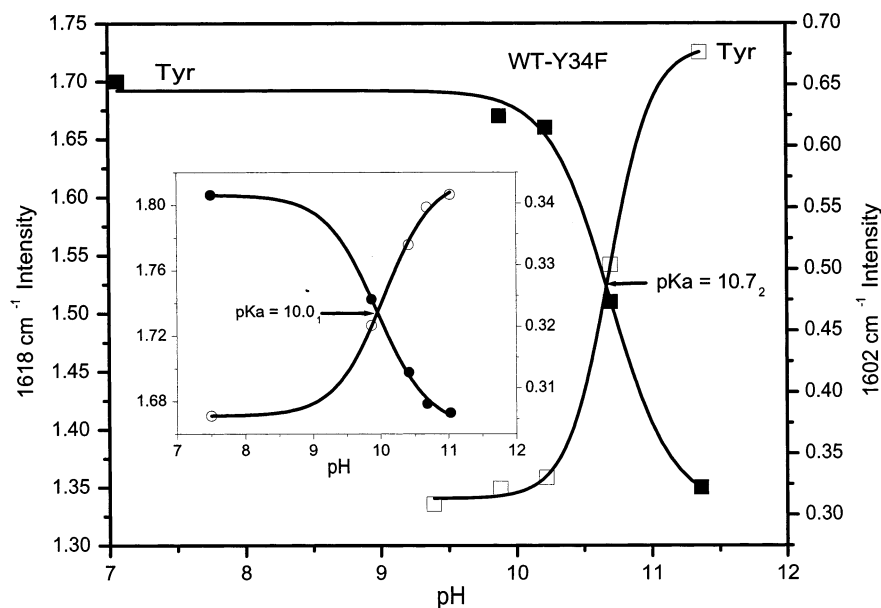
Figure 9. Titration curves derived from the 1618 cm^{-1} (■, Tyr) and 1602 cm^{-1} (□, Tyr$^-$) band intensities (arbitrary units), for WT-Mn^{2+}SOD, and Y34F—Mn^{2+}SOD as an inset, ● = Tyr, O = Tyr$^-$. To isolate the Tyr34 contribution, the WT intensities were corrected by subtracting the Tyr34-free intensity change determined from the Y34F—Mn^{2+}SOD spectra (after correcting for the concentration difference) at each pH. Fits with the Henderson—Hasselbalch equation yield pKs of 10.01 for Y34F—Mn^{2+}SOD and 10.72 for Tyr34 in the WT-Mn^{2+}SOD. The uncertainty in these values is that of the pH reading itself, ± 0.06 units.

intensities, which reflect Tyr34, the difference spectrum shows a pronounced negative W3 band. Thus, the W3 intensity is greater for Y34F—Mn^{2+}SOD than for the WT. The likeliest cause of this effect is enhanced hydrogen bond donation from an indole NH group. Hydrogen bonding is known to augment the W3 intensity because of a red-shift in the excitation profile, as in deoxy-hemoglobin.[58] It is likely that Trp128 is responsible for this effect in MnSOD because its indole NH group donates a hydrogen bond to the side chain carbonyl of Gln146, whose side chain amide in turn donates a hydrogen bond to Tyr34. A notable aspect of the difference W3 band is that its frequency is 10 cm^{-1} lower than the main W3 band of the protein, implying that the Trp residue responsible for the augmented intensity has a lower χ^2 than the remaining Trps. An angle near 90° is predicted by the correlation of Miura et al.[64] Two Trps have χ^2 angles between 70° and 110°: Trp128 and Trp130.

To measure the pKs associated with Tyr residues, we measured the 1618 and 1602 cm^{-1} intensities at several pH values. The intensity vs. pH plots reveal well-behaved single proton titrations (Figure 9). Y34F—Mn^{2+}SOD titrates with a pK of 10.0 and WT-Mn^{2+}SOD displays an additional pK of 10.7. As noted above, the intensity change associated with high pH is smaller for Y34F—Mn^{2+}SOD: the diminution of the 1618 cm^{-1} band is only 8% of the total intensity, whereas for WT-Mn^{2+}SOD, 21% of the intensity is lost in the high pH limit. This behavior implies that Tyr34 contributes much more to the aggregate Tyr intensity than does the residue being titrated in Y34F—Mn^{2+}SOD. Indeed the latter contribution is small enough that the pK = 10.0 step is not apparent in the WT titration data. However, to separate the influence of the titration observed in Y34F—Mn^{2+}SOD from the pH behavior of WT-Mn^{2+}SOD, the change in 1602 or 1618 cm^{-1} intensity observed in Y34F—Mn^{2+}SOD at each pH was subtracted from the intensity observed in WT-Mn^{2+}SOD at that pH, ($I'_{WT} = I_{WT} - \Delta I_{Y34F}$, where I'_{WT} is the adjusted WT intensity, I_{WT} is the raw WT

intensity, and ΔI_{Y34F} is the amount by which the Y34F intensity at the pH of interest differs from Y34F neutral pH intensity), yielding a titration curve for the change due to Tyr34 alone. These curves yield a pK of 10.7 ± 0.1. (Essentially, the same value was obtained from the uncorrected titration curve.)

There are seven Tyr residues in MnSOD, so that Tyr34 contributes 50% more than the average residue to the 1618 cm^{-1} Y8a intensity.[65] As in the case of the Trp W3 band, this augmentation is attributable to a red-shifted excitation profile,[58] indicative of a special hydrogen bonding environment for Tyr34. Indeed, Tyr34 interacts with Gln146, a crystallographic solvent molecule just outside the active site at the base of the channel leading to bulk solvent, and possibly with a water molecule associated with the Mn^{2+} ion (see below). On the other hand, the residue being titrated in Y34F—Mn^{2+}SOD contributes 40% less 1618 cm^{-1} intensity than the average residue. Thus its excitation profile must be blue-shifted instead of red-shifted.

Thus, we assign the large amplitude pK = 10.7 pH dependence observed in WT-Mn^{2+}SOD to Tyr34, consistent with modification of the pK detected by EPR at low temperature[66] in Y34F—Mn^{2+}SOD.

Relation to Published Work. Because the rate constants for the two half reactions of MnSOD are very similar,[15] the pH dependence of K_M reflects the reduced state as well as the oxidized state and the pK of 9.8 exhibited by K_M[19] indicates that both oxidation states should display high pH pKs. Thus, our Mn^{2+}SOD pK near 10.5 is consistent with earlier work. UV resonance Raman data at room temperature indicate that it involves deprotonation of Tyr34. Thus, it resembles Fe^{2+}SOD's pK of 8.5 [43,44] (Scheme 1). Low-temperature Mössbauer

(65) The contribution to the Tyr$^-$ Y8a intensity cannot be quantitated because of the overlap with the neutral Tyr Y8b mode, but it is also much larger than that of the residue being titrated in Y34F—Mn^{2+}SOD.
(66) Attempts to obtain UV resonance Raman spectra on frozen samples were unsuccessful, owing to high background scattering.

Scheme 2. Alternative Possibilities for the Inner-sphere Effect of the PK of Mn^{2+}SOD near pH 10.5
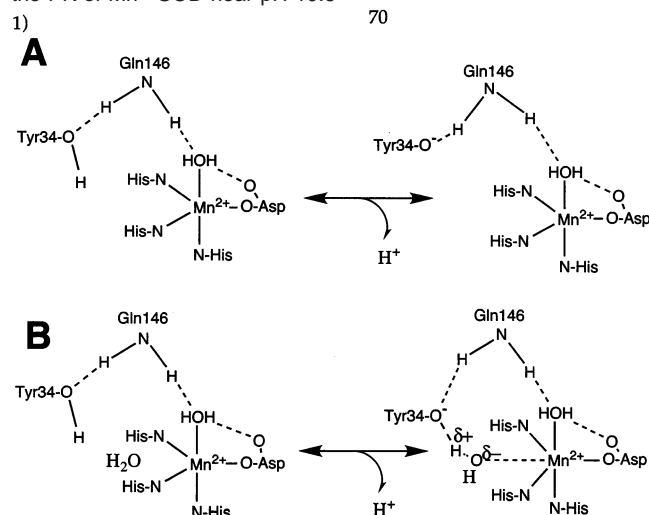
Retention of the His$_3$Asp$^-$ coordination is assumed for simplicity, in the absence of evidence to the contrary.

spectroscopy and MCD indicate that Fe^{2+}SOD's pK does not affect the metal ion coordination sphere[67,68] whereas our low-temperature EPR data indicate that Mn^{2+}SOD's pK does. However, this apparent difference may reflect the exquisite sensitivity of EPR to even relatively subtle perturbations in coordination geometry.

Deprotonation of Tyr and an inner sphere effect are not mutually exclusive, so it simplest to begin by considering that both occur.[69] Deprotonation of Tyr34 could affect the coordination sphere of Mn^{2+} either via the active site hydrogen bond network[12] or via a solvent molecule located between Tyr34 and Mn^{2+} such as that observed crystallographically (Scheme 2, parts A and B, respectively). In the former case, upon deprotonation Tyr34 would become a much better hydrogen bond acceptor, effectively drawing Gln146 away from its less favorable interaction donating a hydrogen bond to already-protonated existing coordinated H$_2$O (Scheme 2A). Even a very slight shift in the position or orientation of Gln146 would thereby conduct proton density toward Tyr34$^-$ at the expense of existing coordinated H$_2$O, thus affecting the EPR signal. Alternately, deprotonated Tyr34$^-$ could polarize additional solvent present between it and Mn^{2+} (Scheme 2B), increasing this solvent's OH$^-$ character as well as occupancy, thus making it better able to interact with Mn^{2+}, and affecting the EPR spectrum. Although the two possibilities are not mutually exclusive, we favor dominance of the former. Binding of F$^-$ or N$_3^-$ leads to smaller zero-field splitting based on their production of significant zero-field intensity in the Mn^{2+}SOD EPR spectrum.[34] Because zero-field intensity represents interdoublet transitions ($m_s = \pm^5/_2 \leftrightarrow m_s = \pm^3/_2$ and $m_s = \pm^3/_2 \leftrightarrow m_s = \pm^1/_2$), it suggests a more symmetric coordination environment (smaller D) and, thus, anion binding as a sixth ligand. In contrast, no new zero-field transitions are observed at high pH (Figure 6) arguing against similar binding of additional OH$^-$ in the sixth position.

Moreover, ionization of existing coordinated solvent is favored in MnSOD by hydrogen bond donation from Gln146 [24,37] (See below and Figure 1).[70]

Mechanistic Implications. The identities and energies of deprotonation events in the active site are important to the mechanism of SOD. Because superoxide is negatively charged, the protonation must be a corequisite or prerequisite for its reduction, yet the pK of O$_2^{\bullet-}$ is 4.7.[71,72] Thus, protonation of O$_2^{\bullet-}$ is probably coupled to its reduction. Moreover, the product of O$_2^{\bullet-}$ reduction at physiological pH is H$_2$O$_2$, with a pK of 11.8.[71,72] Thus, formation of product will be favored by provision of a second proton, which is believed to be rate-limiting in FeSOD.[14] Indeed, both FeSOD and MnSOD are less active at high pH [14,19,46]. However, in FeSOD the pH dependence does not appear to directly reflect lack of a proton destined for product. Instead, the pH dependence of FeSOD activity is interpreted to reflect competitive inhibition of O$_2^{\bullet-}$ binding to Fe^{3+} by OH$^-$ [14,42] and exclusion of O$_2^{\bullet-}$ from the active site upon ionization of Tyr34 in the reduced state[43,44] (Scheme 1).

Similarly, our current assignments of the MnSOD pKs are consistent with the increase in K_M observed at high pH.[19] Because both pKs correspond to deprotonation of Tyr34, and Tyr34 flanks the channel though which substrate is believed to approach the metal ion and bind,[12] ionized Tyr34$^-$ would repel substrate. The fact that k_{cat} does not decrease dramatically at pHs up to 11 [19] indicates that if Tyr34's phenolic proton is transferred to nascent product, this step is not strongly rate-determining. Tyr34's ionizable proton, per se, appears not to be necessary for substrate binding, as the K_M of Y34F−MnSOD is lower than that of WT.[46] k_{cat} is decreased by an order of magnitude in Y34F−MnSOD,[46] but this could reflect an altered reduction potential as well as different local polarity in the substrate binding pocket. Thus, as in Fe^{2+}SOD,[43] Tyr34$^-$ may actively repel anions when deprotonated. This would not incur a significant penalty on activity near neutral pH because Tyr34's pKs are high, but Tyr34 would be mostly ionized at the higher pHs at which hydrogen peroxide becomes significantly deprotonated and seriously inhibitory, Thus, Tyr34's pKs provide a chemical basis for earlier conclusions that Tyr34 confers increased resistance to inactivation by peroxide.[46,47,73]

Finally, the two alternative models for the high pH response of Mn^{2+}SOD's coordination sphere (Schemes 2A and B) would lead to different detailed mechanisms of product inhibition. Our favored model, invoking effective partial deprotonation of existing coordinated H$_2$O at high pH, would constitute partial loss of a proton whose transfer to substrate is required for substrate reduction and/or displacement. Thus, O$_2^{\bullet-}$ might bind but fail to react, or, if O$_2^{-\bullet}$ were to bind and oxidize Mn^{2+}, the resulting O$_2^{2-}$ species could not leave, thus increasing the yield for formation of a peroxo complex, as observed.[26,27,47] In contrast, if the pK were associated with effective increased binding of an additional OH$^-$ to Mn^{2+}, this would exclude inner-sphere substrate binding in the first place, and thus formation

(67) Niederhoffer, E. C.; Fee, J. A.; Papaefthymiou, V.; Münck, E. In *Isotope and Nuclear Chemistry Division, Annual report*; Los Alamos National Laboratory, 1987; pp 79−84.
(68) Jackson, T. A.; Xie, J.; Yikilmaz, E.; Miller, A.-F.; Brunold, T. C. *J. Am. Chem. Soc.* **2002**, accepted.
(69) Their relative importance could nonetheless depend on temperature.

(70) This is also supported by calculations indicating that the pK of the existing coordinated solvent is 3.6 pH units lower in Mn^{2+}SOD than in Fe^{2+}SOD (ref 68).
(71) Ingraham, L. L.; Meyer, D. L. In *Biochemistry of the Elements*; E. Frieden, Ed; Plenum Press: New York and London, 1985; Vol. 4.
(72) Sawyer, D. T. *Oxygen Chemistry*; Oxford University Press, New York, 1991.
(73) Hunter, T.; Ikebukuro, K.; Bannister, W. H.; Bannister, J. V.; Hunter, G. J. *Biochemistry* **1997**, *36*, 4925−4933.

Scheme 3. Effects of Jahn−Teller Distortion on d^5 vs. d^4 or d^6 Centers
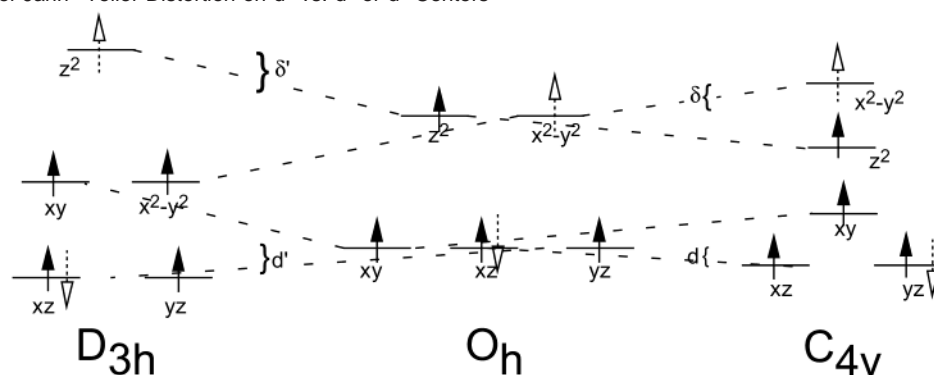
The reference coordination geometry is octahedral (center) and the reference electronic configuration is $d.^5$ The electrons lacking or extra in d^4 or $d,^6$ respectively, are unfilled dashed arrows pointing up or down, respectively. For d^5 systems, the total electronic energy is not changed by distortion to D_{3h} or C_{4v} symmetry, but for d^4 systems, the fact that the destabilized orbital is empty (z^2 for D_{3h} and x^2-y^2 for C_{4v}) results in the system benefitting from net stabilization of δ' or δ. Similarly, for d^6 systems, distortion of the geometry results in stabilization by d' or d.

of any peroxide. Thus, our preferred model is consistent with the favored mechanism of product inhibition, in which endogenously produced peroxide binds to Mn^{3+}.

A. Model Based on Different Jahn−Teller Costs of Coordinating an Additional OH^-. Given the superficial similarity of the FeSOD and MnSOD active sites, it is intriguing that the values and assignments of the pKs are as different as they are. Of the oxidized states, Fe^{3+}SOD's pK corresponds to OH^- binding and expansion of the coordination sphere whereas Mn^{3+}SOD's involves deprotonation of Tyr34 instead. The reduced state pKs of both Fe^{2+}SOD and Mn^{2+} SOD correspond to deprotonation of Tyr34 and subtly perturb the inner sphere but they have values of 8.5 and 10.5, respectively.

The different natures of the oxidized state ionization events of Fe^{3+}SOD and Mn^{3+}SOD could stem in large measure from the different electronic configurations of Fe^{3+} vs. Mn^{3+}. In Mn^{3+}SOD, binding of a sixth ligand comes at the cost of the Jahn−Teller stabilization of the d^4 configuration, however this does not apply to d^5 Fe^{3+}SOD (Scheme 3). Thus, all other factors being equal, Fe^{3+}SOD is expected to have a higher affinity for additional OH^- (lower pK for additional OH^- binding). Even if Tyr34 had the same intrinsic pK of 9.6 in the two systems, more favorable and thus prior binding of OH^- in Fe^{3+}SOD (pK = 8.5) would cause nearby Tyr34's pK to rise significantly. Thus, in Fe^{3+}SOD, ionization of Tyr34 might not be observed below the pH of 11.5 at which Fe^{3+}SOD begins to denature.

By contrast, in a progression from low to high pH, the Mn^{3+} of Mn^{3+}SOD would not bind OH^- as readily so Tyr34 could ionize first, as observed at pH 9.6, and the resulting additional negative charge in the active site adjacent to the substrate access channel would disfavor additional OH^- binding. Thus, the different affinities of Fe^{3+} and Mn^{3+} for a sixth ligand could cause Fe^{3+}SOD and Mn^{3+}SOD to display pKs due to different events, even though both appear to contain "the same" active site Tyr. We note that different values for the effective pKs of individual active site residues may change the roles they play in MnSOD vs. FeSOD.

Fe^{2+}SOD's outer-sphere ionization can also be rationalized in terms of its electronic configuration. Fe^{2+}'s soft nature and d^6 high spin configuration would not favor additional OH^- binding, so Tyr34 would ionize first (as pH is increased) and then Tyr34$^-$ would suppress OH^- binding. Hard, high spin d^5

Mn^{2+} would normally bind an additional OH^- without Jahn−Teller penalty, however we propose that Mn^{2+}'s tendency to be 6-coordinate is sufficiently high that an H_2O molecule *may already be bound* adjacent to Tyr34 at neutral pH, even if only fractionally and weakly. [1] Deprotonation of Tyr34 would be propagated to existing coordinated solvent by the hydrogen bonding network, as well as to the additional solvent. On the basis of our limited data it appears to affect existing coordinated solvent more (above).

Jahn−Teller considerations also correctly predict that Fe-substituted MnSOD (Fe(Mn)SOD) should display an inner-sphere ionization in the oxidized state but an outer sphere ionization in the reduced state. Analogous NMR resonances of the Fe^{2+}(Mn)SOD active site move in the same directions, by similar amounts, as in Fe^{2+}SOD in response to increased pH.[49] This indicates not only that ionization of Tyr34 is responsible, as in Fe^{2+}SOD,[43,44] but also that it has the same effect on the active site. Similarly, both the pK of 8.5−9 of Fe^{3+}SOD [14,42,74] and the pK of 6.1−7 of Fe^{3+}(Mn)SOD[47,49,75,76] appear to correspond to binding of OH^-,[41,42,68,77] although the geometry of the OH^- adducts appear significantly different by EPR.[49] Thus, the (Fe)SOD and (Mn)SOD proteins behave very *similarly* in response to increasing pH when they both contain Fe, supporting the above conclusion that the *different* pH behaviors of FeSOD and MnSOD reflect at least in part their *different* metal ions.

Gln146 as a Bridge between Tyr34 and Existing (Axial) Coordinated Solvent. In addition to the above highly simplified "zero-order" picture, the pH transitions of MnSOD reveal interplay between Tyr34 and the metal center that will modulate the pKs of each. Crystal structures have indicated that the active site Gln links Tyr34 and existing coordinated solvent to other protein residues in a conserved hydrogen bond network.[2,12,46] Tyr34 and Gln69/146 have also been proposed to mediate proton transfer between existing coordinated solvent and bulk solvent.[5,38,47,60] Accordingly, the current findings are consistent with a model in which Gln functions as a hydrogen bonding bridge

(74) Fee, J. A.; McClune, G. J.; Lees, A. C.; Zidovetzki, R.; Pecht, I. *Israel J. Chem.* **1981**, *21*, 54−58.
(75) Yamakura, F.; Kobayashi, K.; Ue, H.; Konno, M. *Eur. J. Biochem.* **1995**, *227*, 700−706.
(76) Yamakura, F.; Matsumoto, T.; Kobayashi, K. In *Frontiers of Reactive Oxygen Species in Biology and Medicine*; Asada, K., Yoshikawa, T., Eds.; Elsevier Science: Amsterdam, 1994; pp 115−118.
(77) Schmidt, M. *Eur. J. Biochem.* **1999**, *262*, 117−126.

Scheme 4. Proposed Relation between the PK of Tyr34 and the Hydrogen Bonding Mediated by Gln69/146, in $Fe^{2+}SOD$ (pK=8.5), $Fe^{2+}(Mn)SOD$ (pK=9.2), $Mn^{3+}SOD$ (pK=9.6) and $Mn^{2+}SOD$ (pK = 10.5)

$Fe^{2+}SOD$, pK = 8.5 $Fe^{2+}(Mn)SOD$, pK = 9.2 $Mn^{3+}SOD$, pK = 9.6 $Mn^{2+}SOD$, pK = 10.5
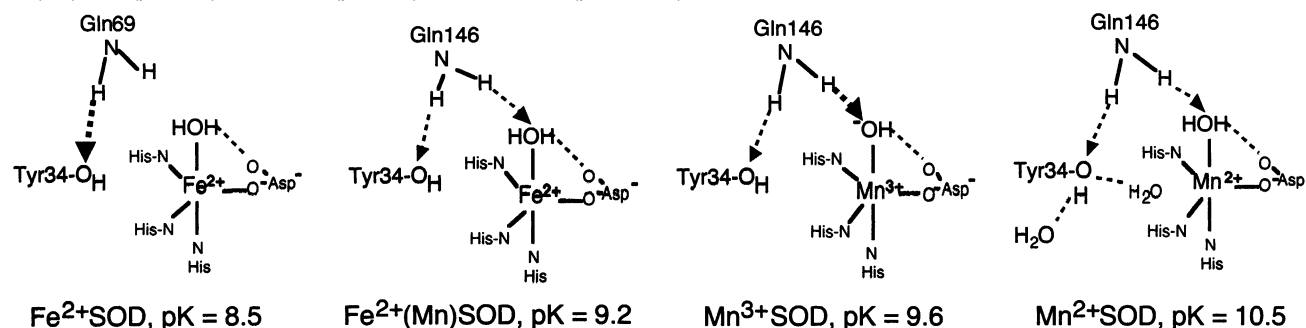
The protein ligands are (counterclockwise from the upper left) His81, His171, His26, and Asp167, and the existing coordinated solvent is shown above the metal ion.

between Tyr34 and existing coordinated solvent. We propose that this bridge is stronger in the MnSOD protein where Gln146 is closer to coordinated solvent[78] and is much more strongly magnetically coupled to Fe^{2+}.[24] Indeed, mutation of Gln146 alters the optical signature of the pK of $Mn^{3+}SOD$, and changes the value of the pK from 9.7 to 10 (for Q146L) and 9 (for Q146H).[60] In addition, Borgstahl's structure [1] and Mn^{2+}'s normal preference for octahedral coordination argue in favor of at least partial presence of an additional H_2O between Tyr34 and Mn^{2+} in $Mn^{2+}SOD$.

The different values of the pK of Tyr34 in the different SOD states can be rationalized in terms of a stronger hydrogen bond network between Tyr34 and coordinated solvent in MnSOD than in FeSOD. Tyr34's pK in $Mn^{2+}SOD$ is 10.5, relatively unperturbed from the solution value, consistent with a high degree of hydration by a conserved crystallographic solvent molecule adjacent to Tyr34 at the base of the channel out to solvent,[2,40] the proposed additional solvent between Tyr34 and Mn^{2+} which should be more highly populated in this state, and hydrogen bond donation from Gln146. This polar environment presumably effectively shields Tyr34 from the nearby net positively charged $[Mn^{2+}(His)_3(H_2O)Asp^-]^{+1}$ site (which is also stabilized by negatively charged Glu170).

By contrast, the pK of Tyr34 in considerably depressed in $Fe^{2+}SOD$ (pK = 8.5 [43,44]), $Fe^{2+}(Mn)SOD$ (pK = 9.2 [49]) and to a lesser extent in $Mn^{3+}SOD$ (pK = 9.3−10.1 [19,45−47]). These are all states in which the metal ion will be less likely to bind additional H_2O based on Jahn−Teller considerations (above) and the variations in the Tyr34 pK are consistent with the Gln bridge model (Scheme 4). In $Mn^{3+}SOD$, Gln146 donates hydrogen bonds to axially coordinated existing OH^- as well as Tyr34. Thus, its capacity as a hydrogen bond donor is shared between two acceptors so Tyr34's pK is depressed, but only slightly. In $Fe^{2+}(Mn)SOD$ the Gln bridge, a feature of the MnSOD protein, is retained but now links Tyr34 to (fully protonated) H_2O as the existing coordinated solvent. Thus, Gln146 is a stronger hydrogen bond donor to Tyr34, explaining the latter's lower pK of 9.2. In $Fe^{2+}SOD$ the existing coordinated solvent is also H_2O but the Gln bridge is essentially disconnected from it (because this is the FeSOD protein). Thus, Gln69's full hydrogen bond donating capacity is devoted to Tyr34, depressing its pK further, to 8.5.

---

(78) Gln N to coordinated solvent O distances are 2.89 Å ± 0.06 in MnSOD (refs 1,40) and 3.41 Å ± 0.08 in $Fe^{3+}SOD$ (ref 2).

Ionization of Tyr34 vs Binding of an Additional OH^-. The same differences in hydrogen bonding and residue positions between the (Fe)SOD and (Mn)SOD proteins can explain the much lower pK for coordination of OH^- as a sixth ligand in $Fe^{3+}(Mn)SOD$ than in $Fe^{3+}SOD$.[47,49,75,76] In MnSOD but not FeSOD, Tyr34 appears to donate a hydrogen bond to N_3^- bound to Mn,[2] which also binds in a different geometry than in FeSOD.[2,25] This could compensate for Mn^{3+}'s innate tendency to not coordinate a sixth ligand, and aid in substrate binding. However when Fe^{3+} replaces Mn^{3+}, the protein's greater participation conspires with the metal ion's greater affinity to favor anion binding. These can explain $Fe^{3+}(Mn)SOD$'s 20-fold higher affinity for N_3^- [47,49] and 2 to 3 order of magnitude higher affinity for OH^-, as compared to $Fe^{3+}SOD$.[47,49,75,76]

Binding of additional OH^- aided by protonated Tyr34, and deprotonation of Tyr34 in the presence of additional H_2O (TyrOH $^-OH \leftrightarrow TyrO^-$ HOH) may represent extremes of a continuum within which subtle perturbations including mutations[47] and change of temperature[53] can modulate the character of the event. Indeed, Tyr34 mutants might still bind additional OH^- but in the absence of assistance from Tyr34 they are expected to do so at higher pH. This could explain the observation in human Y34F−$Mn^{3+}SOD$ of a pK affecting the optical signal but displaced to higher pH.[46,47,60] Indeed, because Y34F−$Mn^{3+}SOD$ began to denature before a high pH asymptote was reached,[46,47] it is not possible to know the value of the pK or the optical spectrum of the high pH species.

Similarly, the pH transitions of $Fe^{3+}SOD$ and $Fe^{2+}SOD$ represent the extremes of an analogous equilibrium. In $Fe^{3+}SOD$ the high pH species has OH^- coordinated to Fe^{3+} as a sixth ligand, but upon reduction this OH^- acquires a proton and dissociates (consistent with the natures of Fe^{2+} vs. Fe^{3+}, above), and Tyr34 is deprotonated (Scheme 1). Thus, in effect Tyr34 has transferred a proton to solvent leaving the sixth position. Finally, an analogous equilibrium could contribute to the temperature dependence of anion binding:

Scheme 5 Alternate polarities of the active site hydrogen bond network.

Conclusions

We have combined a variety of spectroscopic approaches addressing both the Mn center and the nearby conserved Tyr34 of the MnSOD active site, in both oxidation states. This provides a multifaceted description of the events underlying the decrease

Scheme 5. Alternate Polarities of the Active Site Hydrogen Bond Network
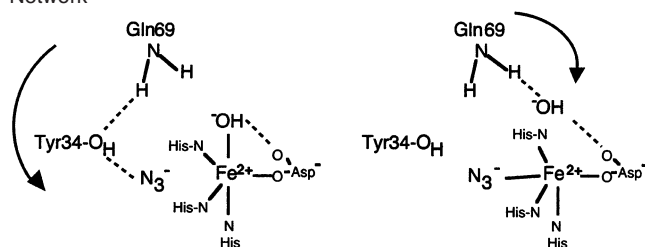
in MnSOD activity near pH 10. We assign the pK near 9.5 in Mn^{3+}SOD and the pK near 10.5 in Mn^{2+}SOD to deprotonation of Tyr34. In both oxidation states the metal center is weakly affected, via the local dielectric, the active site hydrogen bond network and possibly a loosely bound molecule of H$_2$O. While these indirect effects reveal expected parallels between the active sites of FeSOD and MnSOD, the pK assignment in the oxidized state and the different values of Tyr34's pKs in MnSOD vs. FeSOD suggest that details of the mechanisms of the two SODs could be different. They also reinforce earlier suggestions that the Mn center of MnSOD is more intimately coupled to the rest of the protein (and Tyr34) than is the Fe center of FeSOD. This is consistent with the greater E_m depression displayed by the MnSOD protein via stronger hydrogen bonding to the existing coordinated solvent,[24,37] and could reflect the presumed elaboration of a more sophisticated MnSOD in the course of evolution from more primitive FeSOD.